Soft Matter

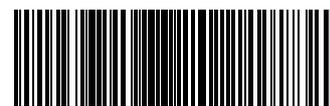Emerging Themes in Soft Matter: Responsive and Active Soft Materials

RSCPublishing

COMMUNICATION
Jennifer A. Lewis *et al.*
Direct-write assembly of biomimetic microvascular networks for efficient fluid transport

PAPER
Yu-Guo Tao and Raymond Kapral
Swimming upstream: self-propelled nanodimer motors in a flow

Direct-write assembly of biomimetic microvascular networks for efficient fluid transport†

Willie Wu,[ab] Christopher J. Hansen,[ab] Alejandro M. Aragón,[bc] Philippe H. Geubelle,[bd] Scott R. White[bd] and Jennifer A. Lewis*[ab]

Biomimetic microvascular networks with complex architectures are embedded in epoxy matrices using direct-write assembly. Fluid transport in multi-generation bifurcating channels is systematically investigated and maximum flow efficiency is found to occur when Murray's law is obeyed.

Nature is replete with examples of vascular networks, whose primary function is the transport of fluid or other substances that promote growth and healing. Typically, these complex networks are composed of hierarchical, bifurcating channels, whose transport efficiency is optimized for a given vascular supply. For example, in blood vasculature, Murray[1] showed that the optimal design equalizes the sum of the radii cubed between the parent and bifurcated child channels, when flow is laminar and the volumetric flow rate is conserved.[2] More recently, McCulloh et al.[3] reported that the architecture of some plant xylem is also well described by this relationship, known as Murray's law. In this case, the xylem architecture maximizes hydraulic conductance, which is beneficial for both internal water transport and photosynthesis.

Considerable attention has been directed towards enhancing the functionality of materials by embedding synthetic microvascular networks. Several emerging applications have been introduced, including self-healing materials,[4,5] 3D[6] and transpiration-based microfluidic devices,[7] tissue engineering scaffolds,[8,9] biomedical devices,[10] and sensors.[11] Due to the complicated architecture of natural vasculature, their replication poses a significant challenge for those pursuing synthetic analogs. Various techniques, including soft lithography,[12–14] laser ablation,[15,16] and direct-write assembly,[6] have been used to create planar and 3D microvascular networks. However, to date, simple networks composed of uniform vascular pathways have mainly been fabricated. In one notable exception, Lim et al.[16] constructed a four-generation, bifurcating network with rectangular channels whose dimensions obeyed Murray's law, but its transport efficiency was not systematically explored.

Here, we create biomimetic microvascular networks of varying microchannel size and hierarchical order and investigate their hydraulic conductance as a function of network design. These networks are patterned by dynamically varying the channel size during direct-write assembly of a fugitive organic ink.[6,17] This critically enabling advance allows the facile construction of multi-generation designs using a single deposition nozzle with a minimum channel diameter of approximately 10 μm.[6] The fugitive ink, a modified form of the wax-based ink reported previously,[6,17] is composed of a mixture of 55% microcrystalline wax (SP19 Strahl and Pitsch) in heavy mineral oil. Under ambient conditions, the ink exhibits strong shear thinning behavior with a low-shear viscosity, η_o, above 10^6 Pa s (Fig. 1a) and a plateau shear storage modulus, G_o', of 10^5 Pa, which decreases when the applied stress exceeds the shear yield stress, τ_y (Fig. 1b). When the

[a]Department of Materials Science and Engineering, University of Illinois at Urbana-Champaign, Urbana, IL, 61801, USA. E-mail: jalewis@illinois.edu
[b]Autonomic Materials Systems Group, Beckman Institute for Advanced Science and Technology, University of Illinois at Urbana-Champaign, Urbana, IL, 61801, USA
[c]Civil and Environmental Engineering Department, University of Illinois at Urbana-Champaign, Urbana, IL, 61801, USA
[d]Department of Aerospace Engineering, University of Illinois at Urbana-Champaign, Urbana, IL, 61801, USA
† Electronic supplementary information (ESI) available: Channel diameters for branched networks and HPFM (high-pressure flow meter) schematic. See DOI: 10.1039/b918436h
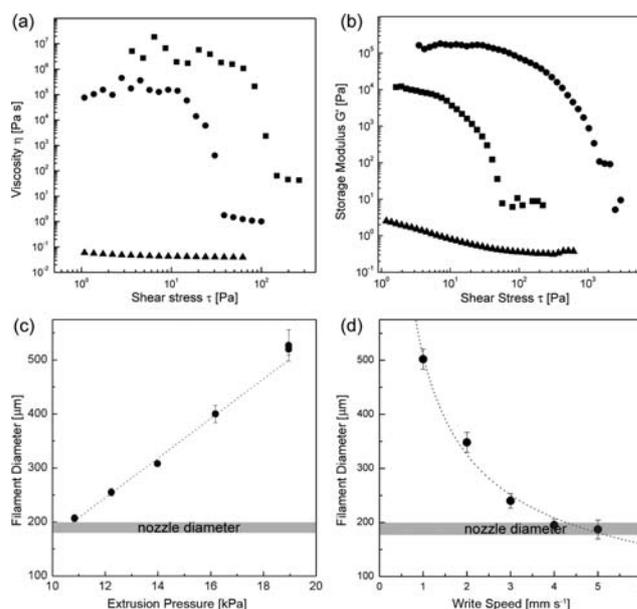

Fig. 1 Fugitive ink rheology and printed filament size. Log–log plot of the ink (a) viscosity η and (b) shear elastic modulus G' vs. stress τ at 25 °C (●), 50 °C (■), and 80°C (▲). Measurements were acquired using a controlled-stress rheometer fitted with a cup and bob geometry oscillating at 1 Hz. (c) Ink filament diameter as a function of applied pressure during direct writing from a cylindrical deposition nozzle (diameter = 200 μm) at 6 mm s⁻¹. The dotted line shows a linear regression of a series of printed calibration rods. (d) Ink filament diameter as a function of writing speed at an applied pressure of 20.1 kPa, where the dotted line shows a power law regression with a scaling exponent of 0.64.

temperature is raised to 50 °C, η_o, G_o', and τ_y are reduced by roughly an order of magnitude. At approximately 80 °C, the ink liquefies leading to a dramatic reduction in its viscosity and, hence, allowing it to be removed from the final structure under a light vacuum, leaving behind the desired microchannel network.

To fabricate biomimetic networks, we modified the direct-write assembly process to enable the facile patterning of hierarchical, bifurcating microchannels. Under normal conditions, the microchannel diameter is roughly equal to the nozzle diameter (D) when the applied pressure (P) and writing speed (v) are controlled such that the volumetric flow rate (Q) equals $0.25\pi D^2 v$. However, this approach would require up to six different nozzles to create the network designs of interest. To simplify the patterning process, we investigated two routes for dynamically varying the ink filament diameter during direct writing. In one route, the applied pressure is varied while the writing speed is held constant (Fig. 1c); in the other route, the applied pressure is held constant, while the writing speed is varied (Fig. 1d). In both cases, a single deposition nozzle (D = 200 μm) is used to create periodic arrays of ink filaments, whose diameters range from 1–2.5D. We find that the printed ink filaments exhibit small variations in size (± 10 μm), when their diameter ranges from 1–1.5D, and larger size variations (± 30 μm) when their diameter exceeds 1.5D. Importantly, it is far easier to dynamically control the ink filament diameter by varying the applied pressure, given the observed linear relationship between these two key parameters. Hence, we implemented this approach for patterning the biomimetic microvascular architectures described below.

To demonstrate the flexibility of our modified assembly technique, we fabricated microvascular networks in the form of a square (90°) lattice, 2-, 4-, and 6-order bifurcating structures, and a 3-order structure that mimics ivy leaf venation. A representative procedure for producing these biomimetic networks is provided in Scheme 1. First, each network is generated using computer-aided design. For the leaf mimic, an image of an English ivy leaf (*Hedera helix* L.) is acquired and its venation pattern is replicated. As described above, the fugitive organic ink is deposited through a cylindrical nozzle into

the desired pattern *via* direct-write assembly.[17] The interstitial pore space between patterned features is then infiltrated with a low-viscosity epoxy resin. Upon curing, the ink is removed leaving behind an interconnected microvascular network for each design of interest.

Three representative microvascular network designs are shown in Fig. 2a–c. All structures are confined to an area of 40×40 mm² and possess a total channel volume of approximately 54 mm³. Each network is patterned by direct-write assembly using a 200 μm nozzle, and then visualized by imbibing a fluorescent dye solution into their interconnected microchannels (Fig. 2d–f). In the square lattice, the microchannels are nominally 200 μm in diameter. By contrast, the 6-order network is composed of microchannels that decrease in size from the parent channel, whose diameter is 530 μm, to the child branches that are nominally 420, 335, 265, 210, 165, and 135 μm in diameter. Finally, the leaf mimic consists of 500, 250, and 100 μm channels. For convenience, we chose to pattern channel sizes that did not conform to the precise dimensions of the natural leaf vascularization.

Scheme 1 Schematic representation of the fabrication procedure for a microvascular network that mimics leaf venation: (a) obtain leaf image; (b) analyze image to identify leaf venation using CAD; (c) deposit fugitive organic ink in the desired pattern *via* direct writing, infiltrate with epoxy resin, and cure to form a structural matrix (individual steps not shown); (d) remove fugitive ink from the matrix leaving behind the desired microvascular network.
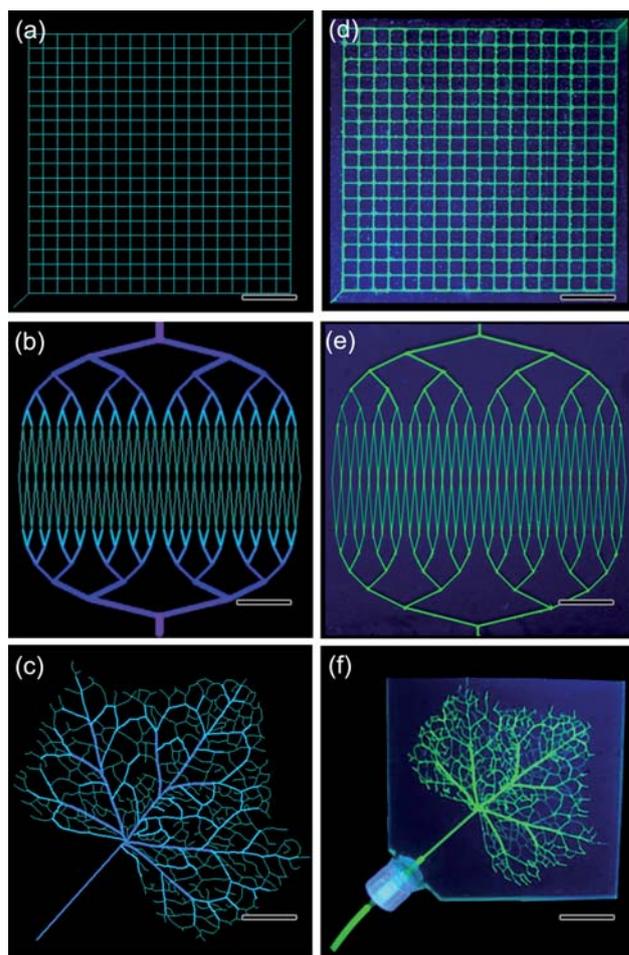

Fig. 2 2D microchannel architectures of varying design. (a–c) Schematic illustrations of 90° lattice, 6-order bifurcating structure following Murray's law, and 3-order structure that mimics ivy leaf venation. Darker blue areas indicate larger channel diameters. (d–f) Corresponding fluorescence images of these microchannel architectures embedded in an epoxy matrix (all scale bars = 10 mm; except (f) whose scale bar = 15 mm).

To systematically investigate the effects of network design on fluid transport efficiency, we constructed a series of 2- and 4-order bifurcating structures and characterized their hydraulic conductance. Henceforth, the 2-order specimens are referred to as Y-networks. A summary of the microchannel diameters patterned for the Y- and 4-order network series is provided in Tables S1 and S2, respectively (see ESI†). Within each series, one network is fabricated that obeys Murray's law, i.e., at each junction $\Sigma r^3_{child}/\Sigma r^3_{parent} = 1$, along with several networks that deviate considerably from this relationship, where $\Sigma r^3_{child}/\Sigma r^3_{parent}$ is varied by an order of magnitude from 0.2–2. Their hydraulic conductance (K), defined as the inverse of the hydraulic resistance (R), is characterized using the high pressure method (HPM), a technique commonly used in botany for characterizing water transport in leaves.[18] The system functions as a voltage divider, in which the flow rate is analogous to current and the pressure is analogous to the electric potential. The microchannel network of interest is connected in series with tubing of known hydraulic resistance (R_1) (see ESI†). A constant pressure is then applied to a reservoir of water that continuously supplies the network, and the system is allowed to reach equilibrium before obtaining the hydraulic resistance. The hydraulic resistance (R_2) of the network is determined by measuring the pressure at the source and between the tubing and the network,

$$R_2 = \frac{P_2 R_1}{P_1 - P_2}, \qquad (1)$$

where P_1 is the pressure at the source, and P_2 is the pressure between the tubing and the microvascular network. We note that this technique is preferable to the direct measurement of the pressure drop across the network, which yields comparable results, but requires longer equilibrium times for these biomimetic microvascular networks.

Due to the simple topological nature of these networks, we derived a closed-form solution for calculating the hydraulic conductance as a function of channel diameters. The total resistance of a bifurcating microvascular network can be derived by considering the contributions of individual segments. For a single channel in a microvascular network undergoing laminar flow, the pressure drop ΔP is related to the volumetric flow rate Q using the Hagen–Poiseuille law:

$$\Delta P = Q\left(\frac{8\mu L}{\pi r^4}\right), \qquad (2)$$

where μ is the dynamic viscosity of the fluid, L is the channel length, and r is the channel radius. The term in parentheses is defined as the hydraulic resistance (R) of the channel. For a simple system consisting of a single bifurcating channel, the analytical solution can be calculated straightforwardly. Because the flow from parent to the child channels is conserved, the flow rate in each of the child channel is half of that of the parent channel. Adding the contributions of parent and simplifying results in the following relation:

$$\Delta P = Q\frac{8\mu}{\pi}\left(\frac{L_0}{r_0^4} + \frac{L_1}{2r_1^4}\right), \qquad (3)$$

where the subscripts denote channel order, with 0 being the parent and subsequent increments indicating the generation of each child. Extending to four generations yields:

$$\Delta P = Q\left[\frac{8\mu}{\pi}\left(\frac{L_0}{r_0^4} + \frac{L_1}{2r_1^4} + \frac{L_2}{4r_2^4} + \frac{L_3}{8r_3^4} + \frac{L_4}{16r_4^4}\right)\right], \qquad (4)$$

where the inverse of the term in the brackets is the hydraulic conductance. We determined appropriate channel radii using the total channel volume (V) and the ratio of parent : child radii (M) as constraints, where:

$$M = \frac{\sum r^3_{i+1}}{\sum r^3_i}, \qquad (5)$$

and i designates channel order. Using this ratio, we can recursively define lower-order microchannels in terms of higher-order channels to obtain a relation that can easily calculate all of the channel diameters given a known total vascular volume (see ESI†). The hydraulic conductance of a network with a given channel ratio is then calculated by substituting into eqn (4) to generate a model curve. The determination of the pressure drop given by eqn (3) and (4) is straightforward due to the simple network geometry and the equal radii of all the branching channels in a given generation. In cases where the configuration of the network is such that a simple formulation cannot be derived, the pressure drop computation requires flow analysis at each channel junction.[19–21] The Hagen–Poiseuille law given by eqn (2) describes the relationship between the pressure drop and the flow rate for a single channel. The flow contribution to the channel endpoints i and j can be expressed as follows:

$$\left\{\begin{array}{c} Q_i \\ Q_j \end{array}\right\} = \frac{\pi r^4}{8\mu L}\left[\begin{array}{cc} 1 & -1 \\ -1 & 1 \end{array}\right]\left\{\begin{array}{c} p_i \\ p_j \end{array}\right\} \qquad (6)$$

Considering the local contributions of n microchannels in the network, a global system of linear equation $KP = C$ is assembled, where K is the global characteristic matrix, P is the network pressure vector and C is the network consumption vector. The system of equations is solved after applying boundary conditions, which involve prescribed consumption and pressure values at inflow and outflow locations, respectively. The maximum pressure drop is then obtained from the pressure vector once the system of equations is solved. This methodology, which verifies the results given by eqn (3) and (4), can be used for computing the hydraulic conductance of more complex architectures.

Fig. 3 shows the predicted and measured values for the hydraulic conductance of the Y- and 4-order microvascular networks. Our results reveal that the maximum hydraulic conductance is obtained when Murray's law is obeyed, in good agreement with prior studies.[3] Interestingly, a much sharper peak in the hydraulic conductance is predicted as the microchannel order increases. Hence, even modest deviations away from Murray's law substantially decrease fluid transport efficiency. Over the range of network designs explored, we find that those conforming to Murray's law exhibit a two-fold enhancement in hydraulic conductance. We further find that the measured values of hydraulic conductance are in reasonably good agreement with the analytical predictions for both the Y- and the 4-order networks. The modest differences observed likely reflect deviations in the printed microchannel diameter as well as defects at the microchannel junctions that arise between two overlapping ink filaments. To quantify this, we created a series of ten identically patterned Y-networks composed of three different $\Sigma r^3_{child}/\Sigma r^3_{parent}$ values and measured their hydraulic conductance. These data, shown as error bars in Fig. 3a, indicated that there is roughly a 15% variation in hydraulic conductance when $\Sigma r^3_{child}/\Sigma r^3_{parent} = 1$. The observed variation increases further to 29% when $\Sigma r^3_{child}/\Sigma r^3_{parent} = 10.25$ and 24% when $\Sigma r^3_{child}/\Sigma r^3_{parent} = 1.75$. Of course, these errors are likely to
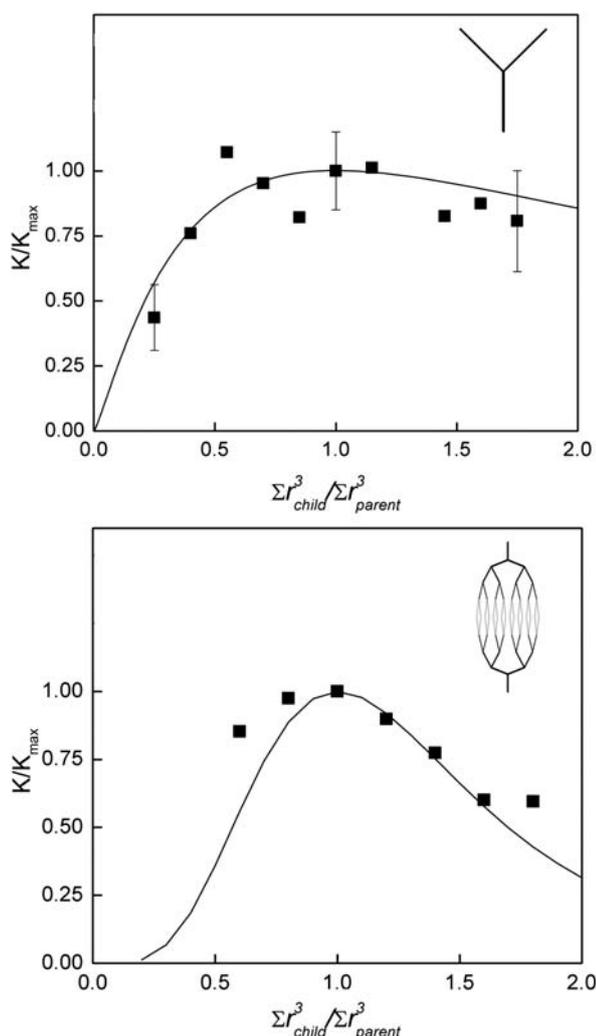
Fig. 3 Normalized hydraulic conductance of hierarchical, bifurcating microchannels normalized to Murray's law maximum plotted as a function of channel architecture for (a) Y-networks and (b) 4-order networks. Analytical solutions for K are shown as solid lines, where K_{max} is given by 1.83×10^{-6} and 4.16×10^{-6} m^3 MPa^{-1} s.

be compounded as the number of generations increases. Nevertheless, given that the pressure drop (ΔP) scales inversely with the channel diameter to the fourth power, the observed deviation between the predicted and measured hydraulic conductance and measurement variability is quite reasonable.

In summary, we have demonstrated that direct-write assembly offers a facile pathway for constructing biomimetic microvascular networks. Our observations support the notion that fluid transport efficiency is maximized when the network architecture obeys Murray's law,[1,3,22–24] in good accord with analytical predictions. The

ability to create biomimetic microvascular networks, coupled with the potential for 3D scalability of this modified direct-write assembly technique, opens new avenues for engineering functional materials for myriad technological applications, including autonomic healing, active cooling, novel microfluidic devices, and tissue engineering. These applications may benefit from hierarchical networks with biomimetic optimization by maximizing the coverage of fluid distribution, while reducing the amount of energy required for pumping.

Acknowledgements

Notes and references

1 C. D. Murray, *Proc. Natl. Acad. Sci. U. S. A.*, 1926, **12**, 207.
2 E. Hagenbach, *Ann. Phys. Chem.*, 1860, **185**, 385.
3 K. A. McCulloh, J. S. Sperry and F. R. Adler, *Nature*, 2003, **421**, 939.
4 K. S. Toohey, N. R. Sottos, J. A. Lewis, J. S. Moore and S. R. White, *Nat. Mater.*, 2007, **6**, 581.
5 C. J. Hansen, W. Wu, K. S. Toohey, S. R. White, N. R. Sottos and J. A. Lewis, *Adv. Mater.*, 2009, **21**, 4143–4147.
6 D. Therriault, S. R. White and J. A. Lewis, *Nat. Mater.*, 2003, **2**, 265.
7 T. D. Wheeler and A. D. Stroock, *Nature*, 2008, **455**, 208.
8 J. T. Borenstein, E. J. Weinberg, B. K. Orrick, C. Sundback, M. R. Kaazempur-Mofrad and J. P. Vacanti, *Tissue Eng.*, 2007, **13**, 1837.
9 A. P. Golden and J. Tien, *Lab Chip*, 2007, **7**, 720.
10 T. Fujii, *Microelectron. Eng.*, 2002, **61–62**, 907.
11 M. L. Chabinyc, D. T. Chiu, J. C. McDonald, A. D. Stroock, J. F. Christian, A. M. Karger and G. M. Whitesides, *Anal. Chem.*, 2001, **73**, 4491.
12 N. W. Choi, M. Cabodi, B. Held, J. P. Gleghorn, L. J. Bonassar and A. D. Stroock, *Nat. Mater.*, 2007, **6**, 908.
13 M. K. Runyon, B. L. Johnson-Kerner, C. J. Kastrup, T. G. Van Ha and R. F. Ismagilov, *J. Am. Chem. Soc.*, 2007, **129**, 7014.
14 J. M. Higgins, D. T. Eddington, S. N. Bhatia and L. Mahadevan, *Proc. Natl. Acad. Sci. U. S. A.*, 2007, **104**, 20496.
15 D. H. Kam and J. Mazumder, *J. Laser Appl.*, 2008, **20**, 185.
16 D. Lim, Y. Kamotani, B. Cho, J. Mazumder and S. Takayama, *Lab Chip*, 2003, **3**, 318.
17 D. Therriault, R. F. Shepherd, S. R. White and J. A. Lewis, *Adv. Mater.*, 2005, **17**, 395.
18 L. Sack, P. J. Melcher, M. A. Zwieniecki and N. M. Holbrook, *J. Exp. Bot.*, 2002, **53**, 2177.
19 A. M. Aragón, C. J. Hansen, W. Wu, P. H. Geubelle, J. A. Lewis and S. R. White, *Proc. SPIE-Int. Soc. Opt. Eng.*, 2009, **6526**, 65261G.
20 C. Brebbia and A. Ferrange, *Computational Hydraulics*, Buttersworths, London, 1983.
21 A. M. Aragón, J. K. Wayer, P. H. Geubelle, D. E. Goldberg and S. R. White, *Comput. Methods Appl. Mech. Eng.*, 2008, **197**(49–50), 4399–4410.
22 K. A. McCulloh and J. S. Sperry, *Tree Physiol.*, 2005, **25**, 257.
23 T. Sherman, *J. Gen. Physiol.*, 1981, **78**, 431.
24 L. A. Taber, S. Ng, A. M. Quesnel, J. Whatman and C. J. Carmen, *J. Biomech.*, 2001, **34**, 121.